PHYSICAL REVIEW B **79**, 121307(R) (2009)

# Rules of peak multiplicity and peak alignment in multiexcitonic spectra of (In,Ga)As quantum dots

Vladan Mlinar, Alberto Franceschetti, and Alex Zunger*
*National Renewable Energy Laboratory, Golden, Colorado 80401, USA*
(Received 27 January 2009; published 27 March 2009)

A simple model—the single-configuration perturbation theory—has traditionally been used to explain the main features of the multiexcitonic spectra of quantum dots, where an electron and a hole recombine in the presence of other $N_e-1$ electrons and $N_h-1$ holes. The model predicts the $(N_h,N_e)$ values for which such spectra consist of a single line or multiple lines and whether singlet lines of different $(N_h,N_e)$ values are energetically aligned. Here we use a nonperturbative, correlated approach that shows when such simple rules work and when they fail, thereby establishing a basis for the appropriate use of such rules.

DOI: 10.1103/PhysRevB.79.121307 PACS number(s): 73.21.La, 78.67.Hc

The remarkable ability to charge semiconductor quantum dots (QDs) by a few electrons or holes and observe multiexciton emission lines[1–5] has provided direct fingerprints of many-particle physics in confined spaces.[4] Loading $N_h$ holes and $N_e$ electrons into a QD creates neutral excitons (if $N_h=N_e$) or charged excitons (if $N_h \neq N_e$). Radiative recombination of one electron with one hole in the presence of $N_h-1$ and $N_e-1$ "spectator" carriers results in a multiexcitonic emission spectrum consisting generally of a few lines. This unique effect is not usually seen in colloidal QDs, where efficient nonradiative Auger recombination of multiexcitons prevents radiative emission.[6]

The basic features of multiexcitonic spectra have been generally interpreted using "single-configuration perturbation theory" (SCPT), i.e., by neglecting correlation effects.[7] In this approach one determines the spectroscopic features by considering only a single configuration (an assignment of electron and hole occupations to electron and hole levels) for the initial and the final states. This widely used perturbative approach results in two remarkable predictions: first, it predicts for which $(N_h,N_e)$ multiexciton system the emission spectrum will consist of a single line ("singlet") or multiple lines ("multiplet"). Second, it predicts when single lines of different $(N_h,N_e)$ multiexciton systems will align energetically ("hidden symmetry").[5] Here we use a general nonperturbative configuration-interaction (CI) calculation, based on atomistic pseudopotential wave functions, to determine the range of validity of SCPT general rules. We find that when obeyed these rules are largely independent of the detailed morphology of the dot. We identify cases where the rules are violated because correlation effects sufficiently modify the wave functions so as to alter the number and alignment of the lines. This study provides a basis for the appropriate use of the SCPT rules.

*The single-configuration perturbation theory approach.* Figure 1 illustrates the expressions for the excitonic recombination energies within the SCPT approximation in terms of the repulsive Coulomb electron-electron ($J_{es,es}$, $J_{es,ep}$, $J_{ep,ep}$, etc.) and hole-hole ($J_{hs,hs}$, $J_{hs,hp}$, $J_{hp,hp}$, etc.) energies, as well as the attractive Coulomb electron-hole ($J_{es,hs}$, $J_{es,hp}$, $J_{ep,hs}$, etc.) energies, where $s$ and $p$ denote orbital character, $e$ is electron, and $h$ is hole. Contributions from electron-electron and hole-hole exchange energies ($K_{es,ep}$, $K_{es,ep2}$, $K_{hs,hp}$, $K_{hs,hp2}$, etc.) are also given in Fig. 1. In this simple SCPT approach one neglects spin-orbit coupling as well as electron-hole exchange energies since $K_{e,h} \ll K_{e,e}$; $K_{h,h}$.[5,8,9] Furthermore, one neglects correlation effects that would allow different configurations to couple. The SCPT also assumes "Aufbau" occupation of electron and hole levels in the initial state.

The SCPT approximation leads to two general predictions: first, the "perturbation theory singlet/multiplet" (PTSM) rule, which determines when a $(N_h,N_e) \rightarrow (N_h-1,N_e-1)$ multiexcitonic spectrum will consist of a single dominant line (singlet) or will exhibit a manifold of lines (multiplet). The PTSM rule states that if in the final state there is a maximum of one partially occupied hole and one partially occupied electron level, then the $(N_h,N_e) \rightarrow (N_h-1,N_e-1)$ spectrum will consist of a single line; otherwise multiple lines are expected. Figure 1 illustrates this prediction for several $(N_h,N_e) \rightarrow (N_h-1,N_e-1)$ transitions by indicating in each panel the term SCPT=singlet or SCPT=multiplet. For example, the final state of the $(4,4) \rightarrow (3,3)$ transition can have one partially occupied $P$-electron level and one partially occupied $P$-hole level ($P_e-P_h$ recombination channel) or one partially occupied $S$-electron level and one partially occupied $S$-hole level ($S_e-S_h$ recombination channel). According to the PTSM rule, both $S_e-S_h$ and $P_e-P_h$ recombination channels will consist of a single line. Applying this rule predicts singlet spectra for $(1,1) \rightarrow (0,0)$, $(2,2) \rightarrow (1,1)$, $(4,4) \rightarrow (3,3)$, and $(6,6) \rightarrow (5,5)$ ($S$ channel); and for $(3,3) \rightarrow (2,2)$, $(4,4) \rightarrow (3,3)$, and $(6,6) \rightarrow (5,5)$ ($P$ channel).[10] Multiplets are expected for $(3,3) \rightarrow (2,2)$ and $(5,5) \rightarrow (4,4)$ ($S$ channel), and for $(5,5) \rightarrow (4,4)$ ($P$ channel).

Second, the expressions shown in Fig. 1 suggest a "perturbation theory peak alignment" (PTPA) rule: under well-defined approximations all singlet transition energies for different $(N_h,N_e) \rightarrow (N_h-1,N_e-1)$ spectra will align. For example, in the SCPT approximation the $(2,2) \rightarrow (1,1)$ transition energy equals the $(1,1) \rightarrow (0,0)$ transition energy plus a correction term $(J_{es,es}+J_{hs,hs})-2J_{es,hs}$ reflecting the balance between Coulomb repulsion of like carriers and Coulomb attraction of unlike carriers. If this term vanishes the $(2,2) \rightarrow (1,1)$ and $(1,1) \rightarrow (0,0)$ singlets will align. This would be the case, e.g., if the electron wave functions were the same as

 

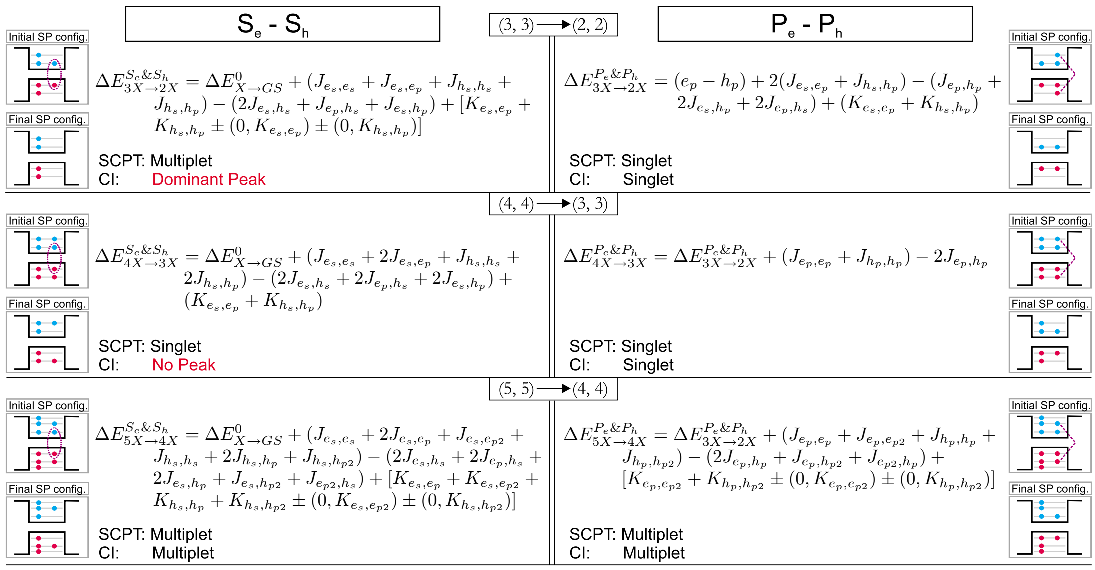


FIG. 1. (Color online) Excitonic recombination energies in the SCPT approximation in terms of electron-electron ($e$-$e$), hole-hole ($h$-$h$), electron-hole Coulomb energies ($J_{es,es}$, $J_{es,ep}$, $J_{hs,hs}$, $J_{es,hs}$, etc.), and $e$-$e$ and $h$-$h$ exchange energies ($K_{es,ep}$, $K_{hs,hp}$, etc.) under the assumption that spin-orbit coupling is negligible. The predictions of the PTSM are compared with those of CI.

the hole wave functions, i.e., $S$-electron orbital equals $S$-hole orbital, $P$-electron orbital equals $P$-hole orbital, etc. In the context of the $P_e - P_h$ channel, this rule was described previously by Bayer *et al.*[5] and by Hawrylak[8] and was referred to as hidden symmetries. The hidden-symmetry rules were originally derived under rather stringent conditions of (i) transitions from and to orbitally degenerate shells (e.g., $P$ and $D$ shells) and (ii) identical $e$-$e$ and $e$-$h$ and $h$-$h$ interactions $V_{ee} = V_{hh} = V_{eh}$.[5,8]

In this work we wish to establish the extent to which the simple PTSM and PTPA rules that emerge from SCPT approximation are borne out by a higher level theory that includes correlation between different configurations. We further discuss the universality of these rules in terms of their dependence on the detailed morphology of the dot.

To this end we calculated the multiexcitonic spectra using a method[7,11] that goes beyond simple counting of interactions: For the assumed size, shape, and composition of a QD we first relax the atomic position $\{\mathbf{R}_{i,\alpha}\}$ via the valence force field method,[12] and construct the total pseudopotential of the system $V(\mathbf{r})$ by superposing the atomic (pseudo)potentials centered at the atomic equilibrium positions for $\sim 2\times 10^6$ atoms: $V(\mathbf{r}) = \Sigma_{i,\alpha} v_\alpha(\mathbf{r}-\mathbf{R}_{i,\alpha})$. The Hamiltonian $-1/2\nabla^2 + V(\mathbf{r}) + V_{\rm so}$ (where $V_{\rm so}$ is the nonlocal spin-orbit interaction) is diagonalized in a basis $\{\phi_{n,\epsilon,\lambda}(\mathbf{k})\}$ of Bloch bands, of band index $n$ and wave vector $\mathbf{k}$, for material $\lambda$ (InAs and GaAs).[11] Multiexciton complexes are calculated using the CI method.[7,13] Slater determinants are constructed from $s$, $p$, and $d$ electron and hole orbitals (well separated in energy from remaining dot-confined states), which give 12 electron and 12 hole single-particle states (counting spin). No symmetry constraints are imposed to these basis states. Coulomb and exchange integrals are computed numerically from the pseudopotential single-particle orbitals. The screening function for these integrals contains an ionic and an electronic component that exhibit a smooth transition from unscreened at short range to screened at long range. Emission spectra are calculated using Fermi's golden rule applied to CI states; configuration mixing in the initial and final states leads to variations in energetic positions and intensities of the emis-

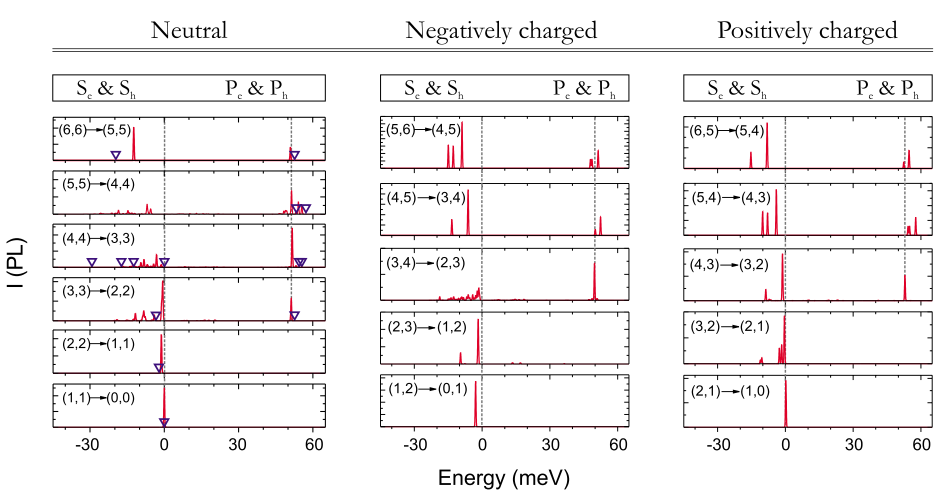


FIG. 2. (Color online) Calculated emission spectra of a lens-shaped $In_{0.6}Ga_{0.4}As/GaAs$ QD, with $2R = 25$ nm and $h = 3.5$ nm for different exciton occupations. Energies are given relative to the monoexciton energy, $E^0_X = 1.255$eV. Gray dashed lines show the position of the $(1,1) \to (0,0)$ monoexciton peak and the position of the $P_e - P_h$ $(3,3) \to (2,2)$ peak. Measured peak positions in the high excitation PL spectra of Ref. 5 are represented by blue open symbols given relative to the measured monoexciton energy, $E^0_X = 1.28$ eV.

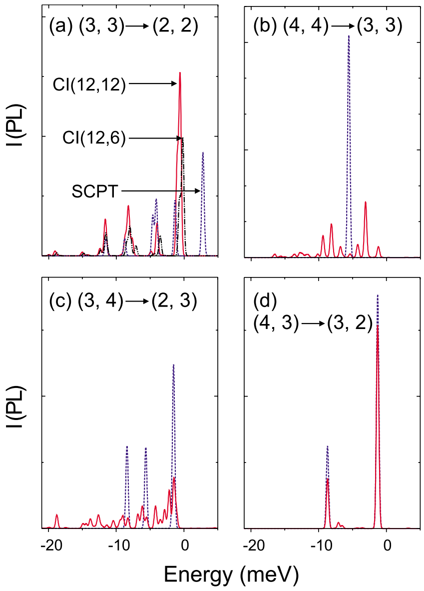


FIG. 3. (Color online) $S_e - S_h$ recombination spectra of (a) (3,3) multiexciton, (b) (4,4), (c) (3,4), and (d) (4,3) multiexcitons, calculated using SCPT (blue dashed curve) and configuration interaction $[\mathrm{CI}(n_h, n_e)]$ depending on number of hole ($n_h$) and electron ($n_e$) states included in the calculations.

sion lines. We first concentrate on flat dots with cylindrically symmetric shape: $\mathrm{In}_{0.6}\mathrm{Ga}_{0.4}\mathrm{As}/\mathrm{GaAs}$ lens-shaped QD with diameter 25 nm and height of 3.5 nm sitting on a 2 ML wetting layer (a range of other shapes is considered below). The calculated multiexcitonic emission spectra are shown in Fig. 2. Measured peak positions in the high excitation PL spectra of Ref. 5 are represented by blue open symbols (dark gray inverted triangles); our results are seen to be in good agreement with the experimental data. Next, we observe that the simple SCPT indeed explains many of the results of the complex calculation. Figure 1 indicates below the PTSM designation also the CI designation, describing the result of the full calculation.

*The singlet/multiplet rule.* We find that the PTSM rule is obeyed by all of the $P$-channel transitions and by the $(1,1) \to (0,0)$, $(2,2) \to (1,1)$, $(5,5) \to (4,4)$, and $(6,6) \to (5,5)$ $S$-channel transitions. There are three exceptions in the case of the $S$-recombination channel.

(i) The PTSM rule predicts a multiplet, but the CI calculation shows a dominant peak: this is the case, for example, of the $(3,3) \to (2,2)$ emission spectrum. Figure 3(a) shows the $S_e - S_h$ recombination spectra of the (3,3) multiexciton calculated using SCPT and CI. In the SCPT approximation the initial state has two electrons in the $S$ level and one in the $P$ level (the same for the holes), so the ground state is: $\Phi^{\mathrm{GS}}_{(3,3)} = h_s^2 h_p^1 e_s^2 e_p^1$. The final state in the $S_e - S_h$ recombination channel has one electron (hole) in the $S$ orbital and one in the $P$ orbital: $\Phi_{(2,2)} = h_s^1 h_p^1 e_s^1 e_p^1$. CI introduces mixing of different configurations. We find that the initial many-particle state of the $(3,3) \to (2,2)$ emission has a dominant $\Phi^{\mathrm{GS}}_{(3,3)}$ character ($\sim 80\%$ weight), while the final state is mostly $\Phi_{(2,2)}$ (60% weight). Configuration mixing leads to one dominant peak compared to the SCPT case, as seen in Fig. 3(a). The ratio between the areas of two most pronounced peaks is 1.78 in the SCPT, while it increases to 4.02 in the CI with a (12,6) basis set and 3.98 with a (12,12) basis set.

(ii) The PTSM rule predicts a singlet, but CI calculations show a multiplet: this is the case, for example, of the $(4,4) \to (3,3)$ emission spectrum. Figure 3(b) shows the $S_e - S_h$ recombination spectrum of the (4,4) multiexciton, calculated using SCPT and CI. According to the PTSM rule, this transition should be a singlet [blue dashed curve in Fig. 3(b)]. The CI calculation, however, shows several peaks of weak intensity. The intensity attenuation is a consequence of the heavily mixed final CI state. The dominant configuration in the final state is indeed $\Phi_{(3,3)} = h_s^1 h_p^2 e_s^1 e_p^2$, but its contribution to the correlated wave function is only 20%.

(iii) The PTSM rule predicts a multiplet, but CI calculations show that the multiplet is actually washed out: this is the case of the $S_e - S_h$ recombination spectrum of the negatively charged multiexciton (3,4), as shown in Fig. 3(c). According to the PTSM rule the $(3,4) \to (2,3)$ emission spectrum should have multiple peaks because there are two partially occupied hole levels in the final state. We find instead that the peaks are suppressed by correlation. The reason for the attenuation of the intensity is the same as in case (ii): the final state is heavily mixed, and although the contribution of the configuration $\Phi^{\mathrm{GS}}_{(2,3)} = h_s^1 h_p^1 e_s^1 e_p^2$ is the largest individually, it is still not the overall dominant configuration. Surprisingly, in the analogous case of the (4,3) positively charged multiexciton there is no attenuation of the emission peaks as both SCPT and CI predict two strong peaks [Fig. 3(d)]. This peculiar result reflects electron-hole asymmetry, a consequence of the lattice asymmetry, strain field, band mixing, intervalley mixing, and spin-orbit interaction.

*The peak alignment rule.* We see from the CI calculation in Fig. 2 that for this particular dot the energies of many of the $(N_h, N_e)$ singlets approximately align. Examples include for the $S_e - S_h$ recombination channel $(1,1) \to (0,0)$ and $(2,2) \to (1,1)$; and for the $P_e - P_h$ recombination channel $(3,3) \to (2,2)$, $(4,4) \to (3,3)$, and $(6,6) \to (5,5)$. Remarkably, this alignment exists even when transitions do not occur from and to orbitally degenerate shells (as required by the hidden-symmetry rule[5]), e.g., there is singlet alignment in the $S_e - S_h$ channel or in the $P$ channel of real structures (see last two columns in Table I) where $P$ shells are never degenerate.

TABLE I. Peak misalignment for $S$- and $P$-recombination channels of five QD structures (see top of Fig. 4). $\Delta_{S_e-S_h}(i,i-1) = \Delta E^{S_e\&S_h}_{iX\to(i-1)X} - \Delta E_{X\to \mathrm{GS}}$, and $\Delta_{P_e-P_h}(i,i-1) = \Delta E^{P_e\&P_h}_{iX\to(i-1)X} - \Delta E^{P_e\&P_h}_{3X\to 2X}$. Last two columns show $P$ shell splitting of electrons ($\delta e_p$) and holes ($\delta h_p$). Energies are given in meV.

| Model dots | $\Delta_{S_e-S_h}$ | | | $\Delta_{P_e-P_h}$ | | $\delta e_p$ | $\delta h_p$ |
|---|---|---|---|---|---|---|---|
| | (2,1) | (3,2) | (6,5) | (4,3) | (6,5) | | |
| Lens-1 | −1.17 | −0.6 | −12.4 | 0.4 | −0.5 | 2.4 | 4.4 |
| Dot A | −1.6 | −1.3 | −12.9 | −0.9 | −0.5 | 3.3 | 0.4 |
| Dot B | −1.5 | −1.5 | −12.7 | −0.9 | −2.0 | 8.9 | 2.4 |
| Dot C | −1.6 | −1.5 | −12.7 | −0.9 | −2.6 | 8.2 | 3.2 |
| Lens-2 | −1.0 | −0.8 | −10.8 | −0.5 | −1.2 | 1.0 | 0.9 |

| Model Dot | Shape | b (nm) | h (nm) | X(In) (%) |
|---|---|---|---|---|
| Lens - 1 | Lens | 25 | 3.5 | 60 |
| Dot A | Truncated pyramid | 25 | 3.5 | 80 |
| Dot B | Elongated lens [1$\bar{1}$0] | 30 | 5.0 | 60 |
| Dot C | Elongated lens [100] | 30 | 5.0 | 60 |
| Lens - 2 | Lens | 30 | 6.0 | 60 |

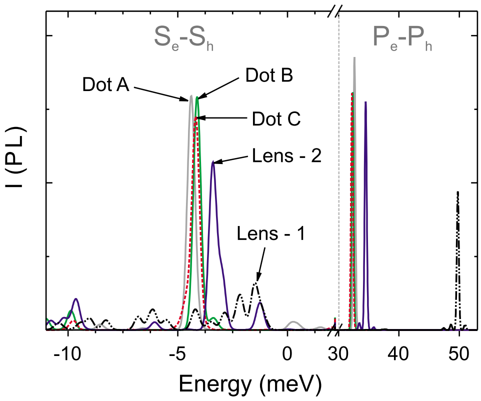


FIG. 4. (Color online) $S$- and $P$-recombination channels of $(3,4)\rightarrow(2,3)$ multiexcitonic transition for five different QD structures, with shape, base length ($b$), height ($h$), and composition [$X$(In)] as shown in top panel. Figs. 1–3 correspond to Lens-1.

Also, the $e$-$e$, $h$-$h$, and $e$-$h$ interactions do not have to be identical to create alignment because of an approximate cancellation of different terms (see expressions in Fig. 1). However, there are also exceptions to the peak-alignment rule; most notably, the singlet $(6,6)\rightarrow(5,5)$ in the $S$ channel does not align with $(1,1)\rightarrow(0,0)$.

*Dependence of the PTSM and PTPA rules on dot structure.* It is natural to enquire if the PTSM and PTPA rules depend on the detailed morphology of the dot or if they are general rules. For this purpose we have constructed several model dots representing a broad range of possibilities, as shown at the top of Fig. 4. (i) Structural dependence vs universality of the PTSM rule: for the $P_e-P_h$ recombination channel, the rule correctly predicts singlets vs multiplets for all QD structures. For the $S_e-S_h$ channel, the PTSM rule does not work for $(3,3)\rightarrow(2,2)$ and $(4,4)\rightarrow(3,3)$ and fails for all dots. The stability of the PTSM rule with respect to QD morphology appears to be an intrinsic feature of $In_xGa_{1-x}As/GaAs$ QDs. Interestingly, the multiexcitonic transition $(3,4)\rightarrow(2,3)$ is particularly sensitive to structural properties, as shown in Fig. 4: the intensity is attenuated in close-to-symmetric flat QDs (lens 1) but increases when increasing the dot height, composition, and base elongation or by modifying the base from circular to square. (ii) Structural dependence vs universality of the PTPA rule: Table I shows the misalignment of singlet peaks defined for the $S_e-S_h$ recombination channel as the distance in energy from the monoexciton $(1,1)\rightarrow(0,0)$ emission ($\Delta_{S_e-S_h}$), and for the $P_e-P_h$ channel as the distance from the $P$-channel $(3,3)\rightarrow(2,2)$ singlet emission ($\Delta_{P_e-P_h}$). Table I shows that $\Delta_{P_e-P_h}\leq 2.6$ meV for the $P$ channel and $\Delta_{S_e-S_h}\leq 1.5$ meV for the $S$ channel, except the singlet of $S_e-S_h$ $(6,6)\rightarrow(5,5)$ which is misaligned by 12 meV. Interestingly, $\Delta_{S_e-S_h}$ and $\Delta_{P_e-P_h}$ do not show significant dependence on QD morphology. Thus, the peak-alignment rule is rather general. This means that observing a singlet line at a given energy does not tell us which multiexciton $(N_h,N_e)$ it is and what QD morphology is involved.

In summary, multiexcitonic transitions can be classified as having a single dominant line or a manifold of lines. All $P_e-P_p$ recombination transitions obey the PTSM rule, whereas there are two exceptions in the case of the $S_e-S_p$ recombination channel: the $(3,3)\rightarrow(2,2)$ transition has only one dominant peak, while the $(4,4)\rightarrow(3,3)$ transitions are attenuated, compared to the predictions of SCPT. We also find that the $(3,4)\rightarrow(2,3)$ transitions are sensitive to structural properties: their intensity is attenuated for close-to-symmetric flat QDs but increases with increasing height, composition, and elongation or by modifying the base from circular to square. Finally, we conclude that the alignment of singlets within the same recombination channel shows almost no sensitivity to QD morphology.

This work was funded by the U. S. Department of Energy, Office of Science under NREL Contract No. DE-AC36-08GO28308.

*alex.zunger@nrel.gov

[1] B. Urbaszek, R. J. Warburton, K. Karrai, B. D. Gerardot, P. M. Petroff, and J. M. Garcia, Phys. Rev. Lett. **90**, 247403 (2003).

[2] J. J. Finley, M. Sabathil, P. Vogl, G. Abstreiter, R. Oulton, A. I. Tartakovskii, D. J. Mowbray, M. S. Skolnick, S. L. Liew, A. G. Cullis, and M. Hopkinson, Phys. Rev. B **70**, 201308(R) (2004).

[3] E. Poem, J. Shemesh, I. Marderfeld, D. Galushko, N. Akopian, D. Gershoni, B. D. Gerardot, A. Badolato, and P. M. Petroff, Phys. Rev. B **76**, 235304 (2007).

[4] M. Ediger, G. Bester, A. Badolato, P. M. Petroff, K. Karrai, A. Zunger, and R. J. Warburton, Nat. Phys. **3**, 774 (2007).

[5] M. Bayer, O. Stern, P. Hawrylak, S. Fafard, and A. Forchel, Nature (London) **405**, 923 (2000).

[6] R. D. Schaller, M. Sykora, J. M. Pietryga, and V. I. Klimov, Nano Lett. **6**, 424 (2006); R. D. Schaller and V. I. Klimov, Phys. Rev. Lett. **96**, 097402 (2006).

[7] A. Franceschetti, H. Fu, L. W. Wang, and A. Zunger, Phys. Rev. B **60**, 1819 (1999).

[8] P. Hawrylak, Physica E **9**, 94 (2001).

[9] P. Hawrylak, Phys. Rev. B **60**, 5597 (1999).

[10] Fine structure splitting of the singlets exists on a much finer energy scale; e.g., for the $(6,6)\rightarrow(5,5)$ singlet, two optically active transitions are split by $\sim$20 $\mu$eV.

[11] L. W. Wang and A. Zunger, Phys. Rev. B **59**, 15806 (1999).

[12] P. N. Keating, Phys. Rev. **145**, 637 (1966).

[13] J. Shumway, A. Franceschetti, and A. Zunger, Phys. Rev. B **63**, 155316 (2001).